Biogeosciences Discuss., 9, 1259–1298, 2012
www.biogeosciences-discuss.net/9/1259/2012/
doi:10.5194/bgd-9-1259-2012

Biogeosciences Discussions

Activity and diversity of methane-oxidizing bacteria in glacier forefields on siliceous and calcareous bedrock

P. A. Nauer[1], B. Dam[2], W. Liesack[2], J. Zeyer[1], and M. H. Schroth[1]

[1]Institute of Biogeochemistry and Pollutant Dynamics, ETH Zurich, 8092 Zurich, Switzerland
[2]Max-Planck-Institute for Terrestrial Microbiology, 35043 Marburg, Germany

Received: 11 January 2012 – Accepted: 13 January 2012 – Published: 30 January 2012

Correspondence to: M. H. Schroth (martin.schroth@env.ethz.ch)

Published by Copernicus Publications on behalf of the European Geosciences Union.

Abstract

The global methane (CH_4) cycle is largely driven by methanogenic archaea and methane-oxidizing bacteria (MOB), but little is known about their activity and diversity in pioneer ecosystems. We conducted a field survey in forefields of 13 receding Swiss glaciers on both siliceous and calcareous bedrock to investigate and quantify CH_4 turnover based on soil-gas CH_4 concentration profiles, and to characterize MOB communities using *pmoA* sequencing and T-RFLP. Methane turnover was fundamentally different in the two bedrock categories. Of the 36 CH_4 concentration profiles from siliceous locations, 11 showed atmospheric CH_4 consumption at concentrations of ~1–2 µl l^{-1} with soil-atmosphere CH_4 fluxes of −0.14 to −1.1 mg m^{-2} d^{-1}. Another 11 profiles showed no apparent activity, while the remaining 14 exhibited slightly increased CH_4 concentrations of ~2–10 µl l^{-1}, most likely due to microsite methanogenesis. In contrast, all profiles from calcareous sites suggested a substantial, yet unknown CH_4 source below our sampling zone, with soil-gas CH_4 concentrations reaching up to 1400 µl l^{-1}. Remarkably, most soils oxidized ~90 % of the deep-soil CH_4, resulting in soil-atmosphere fluxes of 0.12 to 31 mg m^{-2} d^{-1}. MOB showed limited diversity in both siliceous and calcareous forefields: all identified *pmoA* sequences formed only 5 OTUs and, with one exception, could be assigned to either *Methylocystis* or the as-yet-uncultivated Upland Soil Cluster γ (USCγ). The latter dominated T-RFLP patterns of all siliceous and most calcareous samples, while *Methylocystis* dominated in 4 calcareous samples. As Type I MOB are widespread in cold climate habitats with elevated CH_4 concentrations, USCγ might be the corresponding Type I MOBs in habitats exposed to near-atmospheric CH_4 concentrations.

1 Introduction

Methane is a major contributor to recent changes in the global climate system (Forster et al., 2007). Since pre-industrial times, its concentration in the atmosphere has more than doubled, and after appearing to approach a steady state in the early 2000s has continued to rise again to a global average of 1.80 µl l^{-1} (Dlugokencky et al., 2009). Whether influenced by anthropogenic activities or not, the terrestrial CH_4 cycle is largely driven by microorganisms (Conrad, 2009). Methane is produced by strictly anaerobic methanogens that convert products from anaerobic breakdown of organic matter to CH_4 (Conrad, 1996). However, only a fraction of produced CH_4 actually reaches the atmosphere, while a large part is transformed to CO_2 by methane-oxidizing bacteria (MOB) in the transition zone between the anaerobic habitat and the atmosphere (De Visscher et al., 2007; Conrad, 2009). In addition, consumption of atmospheric CH_4 in well-aerated (upland) soils has been observed in all climate zones, including cold environments like tundra, boreal forests and alpine meadows (e.g. Whalen and Reeburgh, 1990; Adamsen and King, 1993; Smith et al., 2000; Flessa et al., 2008; Hartmann et al., 2011). In upland soils, CH_4 uptake seemed to follow Michaelis-Menten kinetics with low K_m-values (Bender and Conrad, 1992). It is hypothesized that specialized "high-affinity" MOB living on trace levels of CH_4 are responsible for this sole terrestrial sink of atmospheric CH_4 (Dunfield, 2007).

Aerobic MOB have been isolated exclusively from environments with elevated CH_4 concentrations. They are Gram-negative and essentially belong to either the γ- or α-proteobacteria (Type I or Type II, respectively; Hanson and Hanson, 1996). Cultivation attempts for high-affinity MOB have been unsuccessful up to now (Kolb, 2009). Evidence of their identity was gained through molecular analyses based on the functional gene *pmoA* that encodes for a subunit of the particulate methane monooxygenase (pMMO). This enzyme catalyzes the first step of CH_4 oxidation, i.e. the conversion of CH_4 to methanol, and is present in almost all known MOB (Hanson and Hanson, 1996; McDonald et al., 2008). Mainly two novel groups of *pmoA* sequences have been

identified in soils consuming atmospheric CH_4. The first group detected, Upland Soil Cluster α (USCα), represents Type-II-related MOB, with *Methylocapsa acidiphila* as their closest cultivated MOB (Holmes et al., 1999; Henckel et al., 2000; Knief et al., 2003; Kolb et al., 2005). They were predominantly found in acidic forest soils. The second group, USCγ, is comprised of *pmoA* sequences most closely related to Type I *Methylococcaceae* and was found in soils with neutral to basic pH values (Knief et al., 2003; Zheng et al., 2011). In addition, *pmoA* from *Methylocystis* was frequently identified in soils oxidizing atmospheric CH_4 (e.g. Knief et al., 2003). Some isolated strains like *Methylocystis* sp. strain SC2 show the capability of growth at CH_4 concentrations of 10 to 100 µl l^{-1} (Knief and Dunfield, 2005; Baani and Liesack, 2008). The ability of strain SC2 to grow at such low CH_4 concentrations is related to the presence of a high-affinity form of pMMO (encoded by *pmoCAB2*). The high-affinity pMMO2 even oxidized methane at atmospheric CH_4 concentrations, contrary to the conventional pMMO1 (encoded by *pmoCAB1*) that oxidized CH_4 only at concentrations above 600 to 700 µl l^{-1} (Baani and Liesack, 2008). It is hypothesized that *Methylocystis* exhibits a "flush-feeding" strategy: it grows and acquires storage compounds during phases of elevated CH_4 concentrations while maintaining cell function with consumption of atmospheric CH_4 (Dunfield, 2007; Kolb, 2009).

Molecular evidence for the presence of *pmoA* provides no information on the magnitude of MOB activity. It is important to accompany molecular ecology techniques by in-situ measurements of CH_4 turnover to assess if MOB are part of the active bacterial community and to provide hands-on information for ecosystem modeling. Most studies investigating CH_4 turnover in situ use the closed-chamber approach and measure CH_4 fluxes across the soil-atmosphere boundary (e.g. Smith et al., 2000). These net fluxes represent a bulk measurement of three underlying processes: physical transport (dominantly diffusion), CH_4 oxidation by MOB and CH_4 production by methanogens. While the conventional chamber method cannot distinguish between the three processes, the soil-CH_4 profile method, i.e. extraction of soil gas at different depths and subsequent analysis of CH_4 concentrations, provides qualitative information about CH_4 production

and consumption zones (Yavitt et al., 1990). Under certain conditions it can also be used to quantify the magnitude of CH_4 oxidation and production (Born et al., 1990; Fechner and Hemond, 1992). Soil physical transport parameters, i.e. the effective diffusion coefficient of CH_4 in soil D_{eff} ($cm^2\ min^{-1}$), can be estimated through concomitant measurement of total soil porosity θ_t and volumetric water content θ_w using empirical relationships (e.g. Kristensen et al., 2010).

Terrestrial CH_4 turnover has been well investigated in developed soils, but surprisingly little is known about magnitude and dynamics of the underlying processes in pioneer ecosystems. In alpine environments, the rapid retreat of many glaciers creates excellent study sites for microbial colonization, diversity and functional strategies (Sigler and Zeyer, 2002; Nemergut et al., 2007; Lazzaro et al., 2009, 2011; Brankatschk et al., 2011). After glacier meltdown, the creation of a well-aerated vadose zone in recently exposed glacier sediments (termed "glacier forefield") might imply an advantage for high-affinity MOB, as they are able to cover their carbon and energy needs from the atmosphere in an otherwise C-limited environment. Additionally, the presence of anoxic conditions in young glacier forefields seems to be widespread (Wadham et al., 2007), which might enhance microsite methanogenesis and opportunistic flush-feeding MOB. Limitations of N in glacier forefields might be overcome by the ability of many MOB to fix N_2 (Auman et al., 2001; Dedysh et al., 2004). Accordingly, a recent study investigating *nifH*-gene diversity of N_2-fixing bacteria in a Swiss glacier forefield affiliated 16 % of total diversity to MOB (Duc et al., 2009).

We therefore hypothesized that glacier forefield soils may exhibit low but measurable consumption of CH_4 through the activity of high-affinity and flush-feeding MOB. To investigate the extent and magnitude of CH_4 oxidation in Swiss Alpine glacier forefields, we conducted a field survey in 13 forefields with different site characteristics. Special attention was given to adequately represent the two main types of subglacial bedrock in the Swiss Alps, siliceous and calcareous, as they exhibit contrasting weathering mechanisms and soil properties (Lazzaro et al., 2009). Specific objectives of the survey were (i) to investigate recently exposed soils in different glacier forefields for CH_4

turnover and quantify CH_4 fluxes using the soil-CH_4 profile method; (ii) to screen these soils for the presence of *pmoA* and investigate the diversity of indigenous MOB with molecular-ecology techniques; and (iii) to characterize sampled forefields in terms of soil physical and chemical properties, and relate potential activity and diversity patterns to relevant parameters.

2 Materials and methods

2.1 Field sites

All sampling took place in summer and autumn 2010 during dry weather conditions. Study sites comprised forefields of 13 receding glaciers in the Swiss Alps (Table 1). Our focus for site selection lay on glaciers that had a forefield with moderate to low steepness featuring fractionated gravel, sand and silt patches, rather than just pure bedrock. The main criteria for choosing sampling locations in each forefield were the possibility of extracting soil gas from depths >30 cm, relatively close proximity to the glacier terminus (~100 to 200 m) and the absence of plant cover. As a consequence mainly of the first criterion, sampled locations throughout all forefields lay in similarly structured patches with minimal skeletal or rock fraction (compared to the rest of the forefield). Hence, although sampled locations are representative only for parts of the respective forefield, they are comparable across sites. Locations are referred to by site abbreviation followed by sampling sequence number (Table 1). Sampled soils may be classified as lithic/skeletic leptosols (IUSS Working Group, 2006), exhibiting a low level of aggregation. The respective soil age (i.e. the duration since exposure to the atmosphere; Table 1) was determined from historical cartographical material (Swiss Federal Office of Topography, Wabern, Switzerland).

2.2 Soil and soil-gas sampling

Soil gas was extracted through a custom-made 2-cm o.d. stainless-steel rod of 80 cm total length, featuring a 1-mm i.d. capillary. The tip of the rod comprised four conical holes of 8 mm o.d., reduced to 1 mm i.d. at 5 mm depth, which were connected to the inner capillary. The rod was gradually hammered into the soil in steps of 5 cm (10 cm after 50 cm depth), until we reached the maximum sampling depth of 70 cm, or hit a boulder. At each step, we extracted 20 ml soil gas with a plastic syringe (after discarding the first 10 ml), then injected it into a gas-tight sampling vial previously N_2-flushed and evacuated. Pressure was measured before and after injection to account for dilution. Due to time constraints and the destructive nature of the sampling procedure, no replicates of soil-gas samples could be taken. Methane was measured on a GC-FID system described in Nauer and Schroth (2010). Oxygen was measured according to Urmann et al. (2007) in samples of the two profiles that showed the highest CH_4 concentrations (WIL 4 and 5).

For molecular and chemical analyses, soil was sampled from 3–10 cm depth, presumably the layer with the highest activity of high-affinity MOB (e.g. Adamsen and King, 1993). Due to low soil aggregation we used spoons, previously washed in commercial bleach and autoclaved, to sample from 4–5 spots in close vicinity to where the soil-gas profile was taken. For each location, the soil was then pooled into one mixed sample and stored on ice until arrival in the lab. For molecular analyses, soil was transferred into a falcon tube and freeze-dried. Fresh soil extracts of 10 g soil in 25 ml 1 M KCl solution and 1 g soil in 10 ml distilled water were prepared and put on an overhead shaker for 1 h and overnight, respectively. The extracts were filtered with 0.45 µm nylon filters and frozen until further analysis. The rest of the sample was dried for 72 h at 60 °C and stored at room temperature.

2.3 Soil physical and chemical properties

After soil and soil-gas sampling had been completed, temperature and θ_w from 0–10 cm depth were measured in the field with a handheld TDR probe (Hydrosense™ System, Campbell Scientific, Logan, UT, USA). For determination of soil bulk density we used an adapted PU-foam method suitable for soils with a high skeletal fraction (Muller and Hamilton, 1992). In a quadratic frame of 12-cm edge length we excavated approx. 1 l of soil to a depth of 10–15 cm. The excavation was then filled with one-component closed-cell PU foam (SOUDAL Mega Schaum, SOUDAL N.V., Turnhout, Belgium) and left to cure for at least 2 h. The volume of the excavation cast was later determined by water displacement. Soil sampled in this way was weighted in the field, then dried in the lab for 72 h at 60 °C for an additional measure of θ_w and particle density, to estimate θ_t and water saturation S_w. We compared the method against a core-sampling procedure in a homogenous sandy soil, where it gave consistent results (standard deviation sd = ±2.5 %). From the same samples we determined grain-size distribution using a laser-diffraction particle-size analyzer (LS 13320, Beckman Coulter Inc., Brea, CA, USA). TDR measurements were erratic and consistently lower than estimated from PU-foam samples, due to the high skeleton fraction of many soils. These values were therefore only used if no PU-foam samples could be taken due to time constraints (i.e. complete curing of the foam was not possible).

The KCl extracts were used to determine soil pH (Soil Survey Staff, 2011) with a Mettler Toledo 830 pH meter (Mettler Toledo, Greifensee, Switzerland), nitrate, sulfate and phosphate by ion chromatography (IC-320, Dionex, Sunnyvale, CA, USA), and ammonium colorimetrically using the protocol of Sims et al. (1995). DOC in the water extracts was determined on a Shimadzu TOC-5000 analyzer (Shimadzu SSI, Columbia, MD, USA) after acidification with 40 µl of 35 % HCl. Total elemental contents, except carbon, were measured by X-ray fluorescence (XRF) analysis (Spectro-X-Lab 2000, Spectro, Kleve, Germany), in pellets of 4 g of milled soil mixed with 0.9 g Hoechst wax. Total carbon (TC) and total inorganic carbon (IC) was measured on a coulometer (CM

5012, UIC Inc., Joliet, IL, USA) using ~10 to 20 mg of milled soil. For TC, the samples were pyrolysed at 950 °C in an autosampler furnace (CM 5200), whereas for IC they were acidified with 2 N perchloric acid in an acidification module (CM 5130). Due to high variance of replicate measurements (sd up to ±0.5 % for siliceous, and ±0.3 % for calcareous samples), organic carbon (OC = TC – IC) was not reported, as computed values were below this threshold.

2.4 DNA extraction and amplification

A total of 27 samples were chosen for molecular analysis, comprising two or three freeze-dried subsamples from each of the 13 sites. The subsamples were chosen according to the greatest differences in CH_4 concentrations at 10 cm depth. The extraction of total DNA was performed using the MP FastDNA® Spin Kit for Soil (MP Biomedicals, Solon, OH, USA), with some minor modifications. Instead of the protein precipitation step as suggested by the manufacturer, the soil homogenate was incubated with proteinase K at 68 °C for 30 min. The DNA was successively extracted with (i) water-saturated phenol, (ii) phenol-chloroform (1:1 [vol/vol]), and (iii) chloroform-isoamyl alcohol (24:1 [vol/vol]). The final supernatant was then mixed with the binding matrix supplied by the MP FastDNA® Spin Kit and the remaining steps were performed as specified in the user manual. DNA yield ranged between 1 to 2 µg (g d.w.)$^{-1}$.

In first-round PCR of *pmoA*, we employed the forward primer A189f in combination with reverse primers A682r, mb661 and A650r (Holmes et al., 1995; Costello and Lidstrom, 1999; Bourne et al., 2001). PCR was run using a touch-down program: initial denaturation (94 °C, 4 min), followed by 10 cycles of denaturation (94 °C, 1 min), primer annealing at 62 °C for 1 min (reduced by 1 °C each cycle to a "touchdown" temperature at 52 °C), and elongation (72 °C, 1 min). Additional 20 cycles were run using the same thermal profile with an annealing temperature of 52 °C. The final elongation step was extended to 7 min. Due to the failure to obtain PCR amplicons from all 27 DNA extracts in the first round, nested PCR was performed with the forward primers A189f and

pmoA206f (Tchawa Yimga et al., 2003) combined with either mb661 or A650r, using 1 µl of the PCR product of primer set A189f-A682r . The thermal profile of second-round PCR consisted of an initial denaturation (94 °C, 4 min), followed by 22 cycles of denaturation (94 °C, 1 min), primer annealing (56 °C, 1 min), and elongation (72 °C, 1 min). PCR amplification was carried out using a reaction mixture containing 1 µl of template DNA, 10 µl of 5 × GoTaq Flexi reaction buffer (Promega, Mannheim, Germany), 1.5 mM $MgCl_2$, 200 mM each dNTP, 5 µg of bovine serum albumin (Promega), 0.5 µM of each primer (A189f/A682 or pmoA206f/mb661), and 2.5 U of Flexi Taq DNA polymerase (Promega). PCR was performed after adjusting the total volume to 50 µl with sterile H_2O, using a DNA thermal cycler (Applied Biosystems, Foster City, CA, USA).

2.5 Analysis of *pmoA* amplicons

Four *pmoA* clone libraries were constructed from composite *pmoA* amplicons generated by nested PCR from FOR 1, GRF 2, MRT 7, and mixed WIL 1, 4 and 5. Cloning was done using the pGEM-T Easy cloning kit (Promega) according to the manufacturer's protocol. In total, 82 *pmoA* sequences were selected for analysis (8 from FOR 1, 21 from GRF 2, 19 from MRT 7, and 35 from WIL 1 + WIL 4 + WIL 5). Cloned inserts (508 bp) were completely sequenced using the BigDye V3.1-terminator chemistry (Applied Biosystems). The identities of the *pmoA* gene sequences were confirmed by searching public sequence databases using nucleotide blast (http://www.ncbi.nlm.nih.gov/BLAST/). Phylogenetic analyses at the DNA and deduced amino acid sequence levels were carried out using the ARB program package (Ludwig et al., 2004). *pmoA* sequences obtained in the course of this study were aligned to a manually curated *pmoA* database containing >3000 sequences. Regions of sequence ambiguity and incomplete data were excluded from the analyses. Results were depicted as a consensus tree, combining the results of Tree-Puzzle, neighbor-joining and maximum likelihood analyses. Representative *pmoA* gene sequences of each species-level OUT

have been deposited in the EMBL, GenBank and DDBJ nucleotide databases under the accession numbers HE647840 to HE647850.

T-RFLP fingerprint patterns were generated in triplicate for each DNA sample. PCR was performed with the forward primer (A189f or pmoA206f) being FAM (6-carboxyfluorescein) -labeled. The *pmoA* PCR products were gel purified by using Wizard SV Gel and PCR Cleanup System (Promega) according to the supplier's protocol. Approximately 100 ng of each *pmoA* amplicon was digested with 10 U of the restriction endonuclease MspI (Promega). The digestion was carried out in a total volume of 10 µl for 12 h at 37 °C. The restriction digests were purified using Illustra AutoSeq G-50 columns (GE Healthcare UK Limited, Little Chalfont, UK). Aliquots (2.5 µl) of the digested amplicons were mixed with 12 µl of deionized formamide (Applied Biosystems) and 0.3 µl of an internal DNA fragment length standard (MapMarker® 1000; BioVentures, Murfreesboro, TN, USA). The mixtures were denatured at 94 °C for 3 min and then chilled on ice. The fluorescently labeled terminal restriction fragments (T-RFs) were size-separated on an ABI 3100 capillary sequencer (Applied Biosystems). The length of each fluorescently labeled T-RF was determined by comparison with the internal standard using GeneScan 3.71 software (Applied Biosystems). The accuracy of size calling between replicates was ±1 bp. The relative abundance of T-RFs in a given T-RFLP pattern was determined as the peak height of the respective T-RF divided by the total peak height of all T-RFs detected within a fragment size range between 50 and 510 bp, and was expressed as percentages (Dunbar et al., 2001; Shrestha et al., 2011).

2.6 Analysis of soil-CH_4 profiles

Methane fluxes J (mg CH_4 m^{-2} d^{-1}) from deep soil (>70 cm) into the sampling zone (J_{ds}), and from there into the atmosphere (J_{atm}), were approximated according to Fick's first law (e.g. Fechner and Hemond, 1992),

$$J \approx D_{\text{eff}} \frac{\Delta C}{\Delta z} \tag{1}$$

where $\Delta C/\Delta z$ is the discrete difference gradient of the 0–5 cm depth interval (J_{atm}), or the two deepest sampling points (J_{ds}), respectively. If the gradient changed direction in the next interval, the mean value of the next three intervals was taken. From θ_t and θ_w we estimated D_{eff} according to the WLR-Marshall model (Moldrup et al., 2000),

$$D_{\text{eff}} = D_{\text{air}} \theta_a^{1.5} \frac{\theta_a}{\theta_t} \tag{2}$$

where D_{air} (14.9 cm^2 min^{-1} at 15 °C and 0.8 bar atmospheric pressure; Fuller et al., 1966) denotes the diffusion coefficient of CH_4 in air, and θ_a is the air-filled porosity of the respective soil ($\theta_a = \theta_t - \theta_w$). Estimated D_{eff} were computed for the first 10 cm of the soil, and assumed to be constant with depth. With this simplification we estimated CH_4 fluxes for profiles showing spatially separated production and consumption zones, and additionally for profiles indicating atmospheric CH_4 consumption.

For profiles indicating atmospheric CH_4 consumption only, a simplified diffusion-consumption model was fitted to measured soil-CH_4 concentrations to estimate first-order rate coefficients k (h^{-1}) of CH_4 oxidation (Born et al., 1990):

$$C_{(z)} = C_{(\infty)} + (C_{(0)} - C_{\infty}) \exp^{-z\sqrt{\frac{k}{D_{\text{eff}}}}} \tag{3}$$

Here, $C_{(z)}$ (µl l^{-1}) denotes CH_4 concentrations at the respective depth z, $C_{(\infty)}$ is the fitted concentration at $z = \infty$, and $C_{(0)}$ is the measured above-ground concentration of CH_4. Eq. (3) was fitted to data using non-linear least squares with a Gauss-Newton algorithm in the *R* environment (*R* 2.11.1; www.r-project.org).

2.7 Statistical analysis

For possible explanations of MOB activity and diversity patterns, we tested individual parameters for significant differences among bedrock types, profile categories and MOB groups (see discussion) using analysis of variance, Pearson's chi-squared test and linear regression in *R*. The explorative design of this survey did not allow a more rigorous statistical analysis to be performed; test statistics served solely the purpose of providing hypotheses for further studies and should not be interpreted conclusively.

3 Results

3.1 Soil properties

Temperatures in 0–10 cm depth varied over a wide range of 4 to 26 °C (Table 2), with highest values measured at STL (16 July), and lowest at DAM (12 October). Sandy soils were the most common, irrespective of bedrock type. Skeleton content was highly variable; at 13 locations it exceeded 50 % (Table 2). Porosities ranged from 0.36 to 0.59, with a mean of 0.45 ± 0.06 (sd), while water saturation ranged from 2 to 37 vol %, with a mean of 16 ± 10 vol % and one outlier of 60 vol %. Computed D_{eff} varied between 1.1 and 4.9 $\mathrm{cm^2\,min^{-1}}$ with a mean of $2.54 \pm 0.87\,\mathrm{cm^2\,min^{-1}}$, not counting one low outlier (0.49) from the location with highest S_{w}, and one high outlier (6.5) from the location with the highest θ_{t} and low S_{w}.

Chemical parameters (site means) are summarized in Table 3. Measured (potential) pH values were generally between 8 and 9 at all calcareous sites, and between 6 and 7.5 at siliceous sites. Exceptional siliceous sites were TSV and MOM, where sampled soils exhibited basic pH values, and DAM, where low pH values of ∼4.9 agreed well with previous findings (Bernasconi et al., 2011). Total carbon was dominated by IC at all calcareous sites (7 to 11 %) and siliceous site TSV (0.3 %), whereas at other siliceous sites TC and IC were in the same low range (0.01 to 0.08 %). Elemental contents of Al,

Fe and P were significantly lower in calcareous sites, on the contrary these soils were enriched in S compared to siliceous sites. Total contents of Cu showed no dependence on site or bedrock type.

Contents of DOC were generally low at all sites (22 to 78 µg $(\mathrm{g\,d.w.})^{-1}$) and showed no significant correlation with site or bedrock type. Concentrations of mineral nitrogen species NH_4^+ and NO_3^- were both significantly enriched at calcareous sites, although concentrations were in the lower µg $(\mathrm{g\,d.w.})^{-1}$ range and close to detection limit. Phosphate was below detection limit (∼0.8 µM) of our instrument at almost all sites, with the exception of BAR and FOR. In accordance with total S contents (Table 3), SO_4^{2-} showed significantly higher concentrations at calcareous sites.

3.2 Soil CH_4 profiles and CH_4 fluxes

Profiles from four sites representing typical situations encountered in this survey are plotted in Fig. 1. At 11 sampled locations in siliceous forefields, soil-gas CH_4 concentrations decreased with depth and showed a curvature, which indicates consumption of atmospheric CH_4 (e.g. BAR 1–4, Fig. 1a). For these locations, lowest measured concentrations ranged between 1.0–1.5 µl $\mathrm{l^{-1}}$. In 11 other profiles from siliceous sites, CH_4 concentrations fluctuated around atmospheric levels (e.g. FOR 1, Fig. 1b). We expect no significant CH_4 turnover at these locations, although we cannot fully exclude the possibility that consumption and production balanced out at the micro-scale level. In 37 of the 59 analyzed profiles, measured soil-gas CH_4 concentrations clearly exceeded atmospheric CH_4 concentrations. At 15 of these locations, all but one (GRF 1) from siliceous sites, highest CH_4 concentrations were only slightly elevated, but always <10 µl $\mathrm{l^{-1}}$, while lowest concentrations could drop below atmospheric levels (e.g. FOR 2, 4 and 5, Fig. 1b). The remaining 22 locations, all from calcareous sites, exhibited soil-gas CH_4 concentrations >10 µl $\mathrm{l^{-1}}$, sometimes by orders of magnitude (e.g. GRF and WIL, Fig. 1c and d). Highest concentrations reached 15 to 130 µl $\mathrm{l^{-1}}$, with the exception of WIL where values up to 1400 µl $\mathrm{l^{-1}}$ were measured. Profile shapes

of most locations clearly indicated a substantial CH_4 source below our sampling zone (hereafter referred to as deep-soil CH_4 source), coupled with CH_4 oxidation in higher soil layers. Note that oxygen concentrations in soil gas from WIL 4 and 5 profiles were close to 20 vol% at all depths (data not shown).

For the 11 profiles exhibiting atmospheric CH_4 consumption, estimated (negative) J_{atm} ranged from −0.14 to −1.1 mg m^{-2} d^{-1}, while k ranged from 0.003 to 29 h^{-1}, with large uncertainties associated with smallest and largest k (Fig. 2). All 18 profiles indicating a deep-soil CH_4 source were net CH_4 emitters, and J_{atm} ranged from 0.12 to 31 mg m^{-2} d^{-1}, with a mean of 6.9 mg m^{-2} d^{-1}. Half of the soils oxidized more than 90 % of the CH_4 before it could reach the atmosphere (Fig. 2). Sink strength of CH_4 oxidation, i.e. the difference between J_{ds} and J_{atm}, was in the range of 2.5 to 240 mg m^{-2} d^{-1}, except for WIL 3–5, where the sink was in the range of 350 to 700 mg m^{-2} d^{-1}.

3.3 *pmoA* presence and diversity analysis

The procedure recommended by the manufacturer (MP Biomedicals) for DNA extraction did not yield a sufficient amount of total DNA from most of our samples. Sufficient amounts were, however, consistently obtained after we replaced the protein precipitation step by a Proteinase K treatment. For initial detection of *pmoA*, we tested the 27 selected DNA extracts with the forward primer A189f in combination with various reverse primers (A650r, mb661r, and A682r). None of the primer combinations consistently produced *pmoA* amplicons from all extracts, but the use of the primer set A189f-A682r resulted in detectable amplicons from 17 locations (Table 4). Nested PCR (with the product of the primer set A189f-A682r) using forward primer A189f in the second round failed, regardless of whether it was combined with A650r or mb661r. However, replacement with pmoA206f (a variant of A189f with 17 additional bases added to its 3′ end) consistently produced detectable *pmoA* amplicons from all the 27 DNA extracts using reverse primer mb661 (Table 4). The combination pmoA206f-A650r again

produced no amplicons. Therefore, for cloning, sequencing and T-RFLP analysis we used primarily *pmoA* amplicons generated in nested PCR with pmoA206f-mb661 in second-round PCR (27 samples representing all 13 sites). First-round PCR amplicons from primers A189f-682r (17 samples from 10 sites) were used for validation of results.

Of the 82 *pmoA* clones randomly selected for analysis, fifty-nine *pmoA* sequences were assigned to *Methylocystis*, while 22 *pmoA* sequences belonged to USCγ. These 81 *pmoA* clone sequences were used to define four species-level operational taxonomic units (OTU-1 to OTU-4) based on 7 % divergence of inferred amino acid sequences (Fig. 3). The *Methylocystis*-like OTU was separated into two subgroups (OTU1a, 1b). The *pmoA* clone sequences of OTU1a are most similar to that of *Methylocystis* sp. M (derived amino acid sequence identity of 98.9 %) and those of the OTU1b (the vast majority) share greatest identity with the *pmoA* of *Methylocystis* strain Rockwell (ATCC 49242; 98.9 %). The three USCγ-like OTUs 2, 3, and 4 are distinct from each other, with identity values of 92 %. Each is most closely related to *pmoA* sequences retrieved from an alpine meadow soil. The single *pmoA* sequence of OTU5 is most closely related to a Cluster I *pmoA* sequence that was detected in deciduous forest soil.

The T-RFLP patterns obtained from all 27 samples by nested PCR can be grouped into two distinct sets of profiles that are dominated by either a 241-bp T-RF or a 243-bp T-RF (Fig. 4). Comparative analysis of *pmoA* clones assigned the 241-bp T-RF to USCγ, while the 243-bp T-RF was highly characteristic of *Methylocystis* (Fig. 3). These assignments were consistently confirmed by in silico analysis of all the 81 *pmoA* clones that had been assigned to either *Methylocystis* or USCγ. The USCγ-related 241-bp T-RF dominated most T-RFLP patterns, including all samples from siliceous sites (Fig. 4). A few T-RFLP patterns (MRT 7, GRI 2, KLG 3 and KLG 4) showed the presence of both the 241-bp and 243-bp T-RFs, with the 241-bp T-RF being always the dominant fragment. The *Methylocystis*-related 243-bp T-RF dominated only in four T-RFLP patterns (GRF 1, GRF 2, WIL 1 and WIL 5), all obtained from calcareous sites.

Besides the dominant 241-bp and 243-bp T-RFs, the T-RFLP profiles showed the presence of two additional T-RFs with a size of 339 and 350 bp. No *pmoA* clone sequences affiliated with these two T-RFs could be obtained. However, in computational analysis using a manually curated database, the 339-bp T-RFs was affiliated with *pmoA* of a particular USC*γ* population, while the 350-bp T-RF appears to represent *pmoA2* of the *Methylocystis*/*Methylosinus* group. These in silico assignments are supported by the consistent co-occurrence of the 241-bp and 339-bp T-RFs and, on the other hand, the 243-bp and 350-bp T-RFs in the T-RFLP patterns (Fig. 4). As suggested by a single *pmoA* clone obtained from sample MRT 7, the 75-bp T-RF found mainly in MRT 6 may represent members of the *pmoA* Cluster 1. The T-RFLP patterns generated from 17 samples by first-round PCR with primers A189f-682r confirmed the dominant presence of either the combination of the 241-bp and 339-bp T-RFs or the 243-bp T-RF (Fig. S1 in the Supplement).

4 Discussion

4.1 Soil properties

Physical properties of the sampled soils varied over a wide range (Table 2), as would be expected from soils in their initial development stage (Egli et al., 2006). However, properties showed no obvious dependence on site characteristics including bedrock type. The majority of soils had a high porosity, and S_w was low as we sampled in dry weather and during the warmest period of the year. Hence, our estimates for D_{eff}, and therefore both J_{atm} and J_{ds} are most likely at the higher end of values that could be expected for glacier forefields.

In general, concentrations of nutrients such as P, N, and DOC were low in glacier forefield soils irrespective of bedrock type (Table 3; Lazzaro et al., 2009, 2011; Bernasconi et al., 2011). Conversely, chemical parameters including pH, total Si, Ca, Al, Fe, S, and IC depended on geology and were significantly different between bedrock

types. As expected for calcareous sites consisting mainly of limestone ($CaCO_3$) and being low in organic carbon, high TC was comprised mainly of IC. Notably, IC and Ca values at individual calcareous sites agreed exceptionally well with each other when taking into account the species' 1:1 stoichiometry in $CaCO_3$ (computations not shown). We tested selected parameters within each bedrock type for correlations with CH_4 turnover and MOB diversity, and discuss them in respective sections below.

4.2 Soil-CH_4 profile categorization

Our initial expectation was that most soils would show CH_4 concentrations slightly below atmospheric levels as a result of atmospheric CH_4 oxidation, with some rare exceptions of slight concentration increases resulting from microsite methanogenesis. Surprisingly, almost two thirds of all measured profiles showed elevated CH_4 concentrations, and around one third of all profiles indicated a substantial deep-soil CH_4 source. To provide an overview of the distribution of dominating processes, we therefore assigned each measured profile to a category according to the generalized shape of the profile (Fig. 5). We distinguished five profile categories that featured the following dominating processes: (A) oxidation of atmospheric CH_4; (B) no apparent CH_4 turnover; (C) small production of CH_4 in anoxic microsites (CH_4 conc. $< 10\,\mu l\,l^{-1}$; limit for growth of cultured oligotrophic MOB; Knief and Dunfield, 2005); (D) substantial deep-soil CH_4 source ($>10\,\mu l\,l^{-1}$) and CH_4 oxidation in the topsoil; (E) substantial CH_4 source ($>10\,\mu l\,l^{-1}$) but undefined profile shape (zig-zag). All profiles from siliceous sites fell into Categories A, B and C, while all profiles from calcareous sites featured a substantial deep-soil CH_4 source and fell into Categories D and E. Given this clear distinction, we discuss the two bedrock types separately below.

Errors in concentration gradients were most likely dominated by local soil heterogeneity, but as no replicate profiles could be taken due to the destructive sampling procedure, we cannot estimate their magnitude. However, having collected several profiles in close proximity, we are confident that our results reflect the general conditions in situ and provide a first estimate of the magnitude of CH_4 turnover in Swiss glacier forefields.

4.2.1 Methane turnover and fluxes at siliceous sites

Considering only siliceous sites, our results support our initial hypothesis of low atmospheric CH_4 consumption (Category A) and limited but prevalent methanogenesis in anoxic microsites (Category C). Bárcena et al. (2010) recently investigated CH_4 oxidation in a (siliceous) glacier forefield in Greenland and found uptake of atmospheric CH_4 in 7 of their 12 sites, with one site at the glacier front emitting CH_4. However, our J_{atm} values were two orders of magnitude higher than their values (−0.0034 to $-0.018\,mg\,m^{-2}\,d^{-1}$), and compared best with the lower end of estimates from cold and temperate ecosystems obtained with similar methods (Born et al., 1990: 0.25–$3.4\,mg\,m^{-2}\,d^{-1}$; Whalen et al., 1992: 0.77–$1.78\,mg\,m^{-2}\,d^{-1}$). Direct comparability with chamber-based net CH_4 fluxes such as reported by Bárcena et al. (2010) is limited, as CH_4 consumption could have been confounded by microsite methanogenesis (Andersen et al., 1998; Kammann et al., 2001, 2009). In glacier forefields, a possible carbon source for methanogenesis might be subfossil wood and peat from glacier-buried vegetation (Hormes et al., 2001). For example, compressed peat disks recovered from the FOR forefield and described in Joerin et al. (2006) could be the origin of localized anoxic conditions due to increased heterotrophic activity at the peat surface.

Profile Categories A, B and C did not significantly differ in S_w but seemed to be temperature-dependent, i.e. temperatures at locations in Category A were significantly lower than in Categories B and C (p-value = 0.025). Similarly, average soil-CH_4 concentrations of "siliceous" profiles were positively correlated with temperature (p-value = 0.0004; $R^2 = 0.35$). Methane-oxidizing bacteria have low temperature sensitivity ($Q_{10} \sim 1$–2; Dunfield et al., 1993; Dunfield, 2007) while methanogens show much higher sensitivity ($Q_{10} \sim 5$–16; Dunfield et al., 1993; Le Mer and Roger, 2001). Possibly, a rather stable activity of MOB might be confounded by increasing methanogenesis at higher temperatures. Soil pH was the only other factor showing a correlation with profile categories, i.e. locations in Category A exhibited significantly lower pH values (p-value = 0.002). Methanogens and MOB occur over wide pH ranges (e.g. Le Mer

and Roger, 2001), but it might be possible that they have different resilience to a gradual decrease in pH occurring during soil development in siliceous glacier forefields (Bernasconi et al., 2011).

4.2.2 Methane turnover and fluxes at calcareous sites

Detection of substantial soil-CH_4 sources at all sampled locations in calcareous glacier forefields was unexpected, as was the magnitude of associated fluxes. At the time of sampling all soils from calcareous sites appeared to be net CH_4 emitters. The range of J_{atm} from locations of Category D compared best with temporarily submerged upland soils (Wang and Bettany, 1997: 7.8–$10.5\,mg\,m^{-2}\,d^{-1}$) and the lower end of estimates from peat bog environments (e.g. Moore and Knowles, 1990: $\sim 5\,mg\,m^{-2}\,d^{-1}$; Fechner and Hemond, 1992: 3.5–$51\,mg\,m^{-2}\,d^{-1}$; Le Mer and Roger, 2001: $43.3\,mg\,m^{-2}\,d^{-1}$, median of 4 sources). Half of the soils of Category D oxidized more than 90 % of J_{ds}, a magnitude usually found in landfill cover soils (De Visscher et al., 2007). This would imply a substantial population of MOB in the most active zone with highest CH_4 turnover, located at ∼50–70 cm depth in most profiles. Unfortunately our soil sampling depth of ∼3–10 cm did not cover this zone; this will be a subject of future investigations.

The nature of the substantial CH_4 source in calcareous glacier forefields remains unknown. Glacially overridden vegetation might directly or indirectly (through relatively labile DOC of subglacial origin; Lafrenière and Sharp, 2004) serve as carbon source for biogenic CH_4 production. Alternatively, cryoconite holes on glacier surfaces have been suggested as relevant sources of organic carbon in glacial ecosystems (e.g. Sawstrom et al., 2002; Hodson et al., 2010; Stibal et al., 2010). In both siliceous and calcareous forefields it is possible that basal ice or permafrost below the vadose zone (note that permafrost is unlikely to exist at our sampling sites; Maisch et al., 2000) might impede drainage and create near-saturated layers that could turn anoxic (Hinkel et al., 2001). However, only on calcareous bedrock a significant loss in soil porosity can occur due to calcite precipitating during freezing (Lacelle, 2007), which could enhance anoxia and hence, methanogenesis. Alternatively, the sedimentary origin of the

calcareous bedrock would also permit a deep geological CH_4 source. Thermogenic CH_4 formed from trapped organic matter might migrate upwards through faults and fractures and result in emission over wide areas ("microseepage"; Matthews, 1996; Etiope and Klusman, 2002). Interestingly, positive microseepage fluxes reported by Klusman et al. (2000) (up to 43 mg CH_4 m^{-2} d^{-1} at the soil-atmosphere boundary) were in the same order of magnitude than our positive J_{atm}. To shed light on the origin of the CH_4 source, we will focus on the determination of the isotopic composition of soil-CH_4 in future work.

From the different parameters tested, only soil temperature showed a correlation with profile categories: temperatures were higher at locations in Category D compared to Category E (p-value = 0.0096). However, measured topsoil temperatures bear little informational value for deep-soil processes. Hence, we cannot provide a meaningful interpretation here.

4.3 *pmoA* presence and diversity of MOB in Swiss glacier forefields

After an initial survey of different primer combinations and PCR conditions, we were able to amplify *pmoA* fragments from all selected 27 subsamples and hence confirm the presence of MOB in all 13 investigated glacier forefields. The key for consistent amplification was a sensitive nested PCR approach and the use of the forward primer pmoA206f, initially designed to specifically detect *pmoA2* (Tchawa Yimga et al., 2003). It seems that *pmoA* variants in our samples shared sufficient nucleotide sequence similarity with *pmoA2* to be efficiently amplified by the nested PCR approach. In contrast with results from a glacier forefield in Greenland (Bàrcena et al., 2010, 2011), amplification with the primer pair A189f-A650R was unsuccessful. Since this primer pair favors the detection of USCα, comparability of their molecular results with this study is limited.

All but one *pmoA* sequences were associated with either *Methylocystis*- or USCγ-like MOB, resulting in a total of only five species-level OTUs. The sequence identity threshold of 7 % in the derived amino-acid sequence corresponds to 87 % nucleotide

sequence divergence for known methanotrophs (Degelmann et al., 2010; Shrestha et al., 2011; Zheng et al., 2011), and correlates with the species-level distance cutoff value of 3 % based on the 16S rRNA gene (Degelmann et al., 2010). Considering the relatively large number of glacier forefields with different climates, altitudes and contrasting geology (Table 1), such a limited number of OTUs is quite surprising. It might be a consequence of the young age of the soils, lack of vegetation and the harsh environmental conditions (e.g. high altitude with strong UV radiation and large temperature shifts) selecting for a few highly specialized MOB.

Although *Methylocystis* was frequently found in environments with low or atmospheric CH_4 concentrations, USCγ has rarely been identified (Knief et al., 2003, 2006; Zheng et al., 2011; Henneberger et al., 2013). Interestingly, the closest related *pmoA* sequences to the three USCγ-OTUs were all retrieved by Zheng et al. (2011) at the same study site, an alpine meadow at the Haibei Ecosystem research station in the Tibetan Plateau. The site has a mean annual temperature of −2 °C, and soils at this site are cryic cambisols typically occurring in permafrost areas. As Type I MOB tend to dominate MOB communities in cold environments (Liebner and Wagner, 2007; Martineau et al., 2010; Yergeau et al., 2010), USCγ might be the corresponding high-affinity MOB dominating upland alpine and arctic soils. The single *pmoA* sequence of OTU5 is most closely related to a Cluster I *pmoA* sequence that was detected in deciduous forest soil, a net sink of atmospheric methane (Knief et al., 2006). It makes sense that this clone was retrieved from MRT 7, the only sample taken in a developing forest where the soil was older than 50 yr.

The two sets of T-RFLP patterns from first- (Fig. S1) and second-round PCR (Fig. 4) compared well. Both sets of patterns consistently show the co-occurrence of the USCγ-assigned 241bp- and 339bp-T-RFs or dominance of the Methylocystis-assigned 243bp T-RF. The co-occurrence of the *Methylocystis*-assigned 243bp-T-RF (*pmoA1*) and 350bp-T-RF (*pmoA2*) can be observed only in the patterns from second-round PCR, because *pmoA2* is not efficiently amplified by the primer pair A189f-A682r used in first round. We are therefore confident that the nested PCR approach generated a

representative picture of MOB diversity in sampled glacier forefields. The relative abundances of the T-RFs in Fig. 4 corroborated the low diversity in the *pmoA* sequences and reflected the strong dominance of USCγ. Surprisingly, USCγ dominated even in sites with acidic pH (DAM and MRT), while in previous studies this group was primarily detected in neutral soil (Knief et al., 2003; Zheng et al., 2011). The occurrence of *Methylocystis* was restricted to calcareous sites. Accordingly, CH_4 concentrations at sampling depth (10 cm) were significantly higher for *Methylocystis*-dominated locations (p-value = 0.0019; including all 27 samples). Growth of isolated strains of *Methylocystis* was restricted to CH_4 concentrations >10 $\mu l\,l^{-1}$ (Knief and Dunfield, 2005; Baani and Liesack, 2008). This would explain the limitation of *Methylocystis* to calcareous sites. As *Methylocystis* might have the ability to express different pMMO isozymes for low (~2–600 $\mu l\,l^{-1}$) and high (>600 $\mu l\,l^{-1}$) CH_4 concentrations (Baani and Liesack, 2008), one would also imply an advantage over USCγ at higher CH_4 availability. However, *Methylocystis*-dominated GRF 1 and 2 showed CH_4 concentrations much lower than 10 $\mu l\,l^{-1}$ in 10 cm depth, and the USCγ-dominated WIL 4 exhibited the highest CH_4 concentrations of all sites. Therefore, with the current data set we cannot give a confident explanation for the occurrence of USCγ or *Methylocystis* at calcareous sites. However, it should be noted that soil-CH_4 concentrations and fluxes likely exhibit diurnal and seasonal variability not reflected by our one-time measurements (Friborg et al., 1997; Hendriks et al., 2010). Second, for most calcareous locations the active zone (largest shift in CH_4 gradient) was much deeper than our sampled depth of 3–10 cm. It will be interesting to analyze *pmoA* diversity and abundance together with CH_4 concentrations in a vertical profile.

5 Conclusions

Our results confirmed the presence of MOB in all sampled Swiss glacier forefields, while MOB activity was evident at many locations. Siliceous and calcareous forefields showed clearly different CH_4 turnover patterns: while atmospheric CH_4 oxidation

accompanied by microsite methanogenesis was common at siliceous sites, all calcareous glacier forefields featured a deep-soil CH_4 source of unknown origin, with MOB consuming up to 90 % of CH_4 before reaching the atmosphere. However, diversity of MOB was limited in both siliceous and calcareous forefields, and was strongly dominated by the USCγ group, which might be widespread in alpine/arctic permafrost environments.

Supplementary material related to this article is available online at: http://www.biogeosciences-discuss.net/9/1259/2012/bgd-9-1259-2012-supplement.pdf.

Acknowledgements. We would like to thank Andreas Gauer, Isolde Erny and Martin Vogt, among others, for their invaluable help with field work. Bomba Dam is grateful to the Alexander von Humboldt Foundation for his fellowship. This project was funded by ETH Zurich (in part through grant no. TH-20 06-3), the Swiss National Science Foundation (grant no. 200021-137721), and the LOEWE Research Center for Synthetic Microbiology (SYNMIKRO).

References

Adamsen, A. P. S. and King, G. M.: Methane consumption in temperate and subarctic forest soils: Rates, vertical zonation, and responses to water and nitrogen, Appl. Environ. Microb., 59, 485–490, 1993.

Andersen, B. L., Bidoglio, G., Leip, A., and Rembges, D.: A new method to study simultaneous methane oxidation and methane production in soils, Global Biogeochem. Cy., 12, 587–594, 1998.

Auman, A. J., Speake, C. C., and Lidstrom, M. E.: *nifH* sequences and nitrogen fixation in type I and type II methanotrophs, Appl. Environ. Microb., 67, 4009–4016, 2001.

Baani, M. and Liesack, W.: Two isozymes of particulate methane monooxygenase with different methane oxidation kinetics are found in *Methylocystis* sp. strain SC2, P. Natl. Acad. Sci. USA, 105, 10203–10208, 2008.

Bárcena, T. G., Yde, J. C., and Finster, K. W.: Methane flux and high-affinity methanotrophic diversity along the chronosequence of a receding glacier in Greenland, Ann. Glaciol., 51, 23–31, 2010.
Bárcena, T., Finster, K., and Yde, J.: Spatial patterns of soil development, methane oxidation, and methanotrophic diversity along a receding glacier forefield, southeast Greenland, Arct. Antarct. Alp. Res., 43, 178–188, 2011.
Bender, M. and Conrad, R.: Kinetics of CH_4 oxidation in oxic soils exposed to ambient air or high CH_4 mixing ratios, FEMS Microbiol. Lett., 101, 261–270, 1992.
Bernasconi, S. M., Bauder, A., Bourdon, B., Brunner, I., Bünemann, E., Chris, I., Derungs, N., Edwards, P., Farinotti, D., Frey, B., Frossard, E., Furrer, G., Gierga, M., Göransson, H., Gülland, K., Hagedorn, F., Hajdas, I., Hindshaw, R., Ivy-Ochs, S., Jansa, J., Jonas, T., Kiczka, M., Kretzschmar, R., Lemarchand, E., Luster, J., Magnusson, J., Mitchell, E. A. D., Venterink, H. O., Plötze, M., Reynolds, B., Smittenberg, R. H., Stähli, M., Tamburini, F., Tipper, E. T., Wacker, L., Welc, M., Wiederhold, J. G., Zeyer, J., Zimmermann, S., and Zumsteg, A.: Chemical and biological gradients along the Damma glacier soil chronosequence, Switzerland, Vadose Zone J., 10, 867–883, 2011.
Born, M., Dörr, H., and Levin, I.: Methane consumption in aerated soils of the temperate zone, Tellus B, 42, 2–8, 1990.
Bourne, D. G., McDonald, I. R., and Murrell, J. C.: Comparison of *pmoA* PCR primer sets as tools for investigating methanotroph diversity in three Danish soils, Appl. Environ. Microb., 67, 3802–3809, 2001.
Brankatschk, R., Towe, S., Kleineidam, K., Schloter, M., and Zeyer, J.: Abundances and potential activities of nitrogen cycling microbial communities along a chronosequence of a glacier forefield, ISME J., 5, 1025–1037, 2011.
Conrad, R.: Soil microorganisms as controllers of atmospheric trace gases (H_2, CO, CH_4, OCS, N_2O, and NO), Microbiol. Rev., 60, 609–640, 1996.
Conrad, R.: The global methane cycle: Recent advances in understanding the microbial processes involved, Environ. Microbiol. Reports, 1, 285–292, 2009.
Costello, A. M. and Lidstrom, M. E.: Molecular characterization of functional and phylogenetic genes from natural populations of methanotrophs in lake sediments, Appl. Environ. Microb., 65, 5066–5074, 1999.
De Visscher, A., Boeckx, P., and van Cleemput, O.: Artificial methane sinks, in: Greenhouse gas sinks, edited by: Reay, D. S., Hewitt, C. N., Smith, K. A., and Grace, J., CABI, Wallingford,

184–200, 2007.
Dedysh, S. N., Ricke, P., and Liesack, W.: NifH and NifD phylogenies: an evolutionary basis for understanding nitrogen fixation capabilities of methanotrophic bacteria, Microbiology (SGM), 150, 1301–1313, 2004.
Degelmann, D. M., Borken, W., Drake, H. L., and Kolb, S.: Different atmospheric methane-oxidizing communities in European beech and Norway spruce soils, Appl. Environ. Microb., 76, 3228–3235, 2010.
Dlugokencky, E., Bruhwiler, L., White, J., Emmons, L., Novelli, P., Montzka, S., Masarie, K., Lang, P., Crotwell, A., and Miller, J.: Observational constraints on recent increases in the atmospheric CH_4 burden, Geophys. Res. Lett., 36, L18803, doi:10.1029/2009GL039780, 2009.
Duc, L., Noll, M., Meier, B., Bürgmann, H., and Zeyer, J.: High diversity of diazotrophs in the forefield of a receding alpine glacier, Microb. Ecol., 57, 179–190, 2009.
Dunbar, J., Ticknor, L. O., and Kuske, C. R.: Phylogenetic specificity and reproducibility and new method for analysis of terminal restriction fragment profiles of 16S rRNA genes from bacterial communities, Appl. Environ. Microb., 67, 190–197, 2001.
Dunfield, P. F.: The soil methane sink, in: Greenhouse gas sinks, edited by: Reay, D., Hewitt, K., Smith, K., and Grace, J., CABI, Wallingford, 152–170, 2007.
Dunfield, P., Knowles, R., Dumont, R., and Moore, T. R.: Methane production and consumption in temperate and subarctic peat soils: Response to temperature and pH, Soil Biol. Biochem., 25, 321–326, 1993.
Egli, M., Wernli, M., Kneisel, C., and Haeberli, W.: Melting glaciers and soil development in the proglacial area Morteratsch (Swiss Alps): I. Soil type chronosequence, Arct. Antarct. Alp. Res., 38, 499–509, 2006.
Etiope, G. and Klusman, R. W.: Geologic emissions of methane to the atmosphere, Chemosphere, 49, 777–789, 2002.
Fechner, E. J. and Hemond, H. F.: Methane transport and oxidation in the unsaturated zone of a Sphagnum peatland, Global Biogeochem. Cy., 6, 33–44, 1992.
Flessa, H., Rodionov, A., Guggenberger, G., Fuchs, H., Magdon, P., Shibistova, O., Zrazhevskaya, G., Mikheyeva, N., Kasansky, O. A., and Blodau, C.: Landscape controls of CH_4 fluxes in a catchment of the forest tundra ecotone in northern Siberia, Glob. Change Biol., 14, 2040–2056, 2008.
Forster, P., Ramaswamy, V., Artaxo, P., Berntsen, T., Betts, R., Fahey, D. W., Haywood, J., Lean,

J., Lowe, D. C., Myhre, G., Nganga, J., Prinn, R., Raga, G., Schulz, M., and Van Dorland, R.: Changes in atmospheric constituents and in radiative forcing, in: Climate change 2007: The physical science basis. Contribution of working group I to the fourth assessment report of the intergovernmental panel on climate change, edited by: Solomon, S., Qin, D., Manning, Z., Chen, Z., Marquis, M., Averyt, K. B., Tignor, M., and Miller, H. L., Cambridge University Press, Cambridge, UK and New York, NY, USA, 2007.

Friborg, T., Christensen, T. R., and Søgaard, H.: Rapid response of greenhouse gas emission to early spring thaw in a subarctic mire as shown by micrometeorological techniques, Geophys. Res. Lett., 24, 3061–3064, 1997.

Fuller, E. N., Schettler, P. D., and Giddings, J. C.: New method for prediction of binary gas-phase diffusion coefficients, Ind. Eng. Chem., 58, 18–27, 1966.

Hanson, R. and Hanson, T.: Methanotrophic bacteria, Microbiol. Mol. Biol. R., 60, 439–471, 1996.

Hartmann, A., Buchmann, N., and Niklaus, P.: A study of soil methane sink regulation in two grasslands exposed to drought and N fertilization, Plant Soil, 342, 265–275, 2011.

Henckel, T., Jackel, U., Schnell, S., and Conrad, R.: Molecular analyses of novel methanotrophic communities in forest soil that oxidize atmospheric methane, Appl. Environ. Microb., 66, 1801–1808, 2000.

Hendriks, D. M. D., van Huissteden, J., and Dolman, A. J.: Multi-technique assessment of spatial and temporal variability of methane fluxes in a peat meadow, Agr. Forest Meteorol., 150, 757–774, 2010.

Henneberger, R., Lüke, C., Mosberger, L., and Schroth, M. H.: Structure and function of methanotrophic communities in a landfill-cover soil, FEMS Microbiol. Ecol., online first: doi:10.1111/j.1574-6941.2011.01278.x, 2012.

Hinkel, K. M., Paetzold, F., Nelson, F. E., and Bockheim, J. G.: Patterns of soil temperature and moisture in the active layer and upper permafrost at Barrow, Alaska: 1993–1999, Global Planet. Change, 29, 293–309, 2001.

Hodson, A., Boggild, C., Hanna, E., Huybrechts, P., Langford, H., Cameron, K., and Houldsworth, A.: The cryoconite ecosystem on the greenland ice sheet, Ann. Glaciol., 51, 123–129, 2010.

Holmes, A. J., Costello, A., Lidstrom, M. E., and Murrell, J. C.: Evidence that particulate methane monooxygenase and ammonia monooxygenase may be evolutionarily related, FEMS Microbiol. Lett., 132, 203–208, 1995.

Holmes, A. J., Roslev, P., McDonald, I. R., Iversen, N., Henriksen, K., and Murrell, J. C.: Characterization of methanotrophic bacterial populations in soils showing atmospheric methane uptake, Appl. Environ. Microb., 65, 3312–3318, 1999.

Hormes, A., Müller, B. U., and Schlüchter, C.: The Alps with little ice: Evidence for eight holocene phases of reduced glacier extent in the central Swiss Alps, Holocene, 11, 255–265, 2001.

IUSS Working Group WRB: World reference base for soil resources 2006, World Soil Resources Reports No. 103, FAO, Rome, 2006.

Joerin, U. E., Stocker, T. F., and Schlüchter, C.: Multicentury glacier fluctuations in the Swiss Alps during the Holocene, Holocene, 16, 697–704, 2006.

Kammann, C., Grünhage, L., Jäger, H. J., and Wachinger, G.: Methane fluxes from differentially managed grassland study plots: The important role of CH_4 oxidation in grassland with a high potential for CH_4 production, Environ. Pollut., 115, 261–273, 2001.

Kammann, C., Hepp, S., Lenhart, K., and Müller, C.: Stimulation of methane consumption by endogenous CH_4 production in aerobic grassland soil, Soil Biol. Biochem., 41, 622–629, 2009.

Klusman, R. W., Leopold, M. E., and LeRoy, M. P.: Seasonal variation in methane fluxes from sedimentary basins to the atmosphere: Results from chamber measurements and modeling of transport from deep sources, J. Geophys. Res., 105, 24661–24670, 2000.

Knief, C. and Dunfield, P. F.: Response and adaptation of different methanotrophic bacteria to low methane mixing ratios, Environ. Microbiol., 7, 1307–1317, 2005.

Knief, C., Lipski, A., and Dunfield, P. F.: Diversity and activity of methanotrophic bacteria in different upland soils, Appl. Environ. Microb., 69, 6703–6714, 2003.

Knief, C., Kolb, S., Bodelier, P. L. E., Lipski, A., and Dunfield, P. F.: The active methanotrophic community in hydromorphic soils changes in response to changing methane concentration, Environ. Microbiol., 8, 321–333, 2006.

Kolb, S.: The quest for atmospheric methane oxidizers in forest soils, Environ. Microbiol. Reports, 1, 336–346, 2009.

Kolb, S., Knief, C., Dunfield, P. F., and Conrad, R.: Abundance and activity of uncultured methanotrophic bacteria involved in the consumption of atmospheric methane in two forest soils, Environ. Microbiol., 7, 1150–1161, 2005.

Kristensen, A. H., Thorbjørn, A., Jensen, M. P., Pedersen, M., and Moldrup, P.: Gas-phase diffusivity and tortuosity of structured soils, J. Contam. Hydrol., 115, 26–33, 2010.

Lacelle, D.: Environmental setting, (micro)morphologies and stable C-O isotope composition of cold climate carbonate precipitates – A review and evaluation of their potential as paleoclimatic proxies, Quaternary Sci. Rev., 26, 1670–1689, 2007.
Lafrenière, M. and Sharp, M.: The concentration and fluorescence of dissolved organic carbon (DOC) in glacial and nonglacial catchments: Interpreting hydrological flow routing and DOC sources, Arct. Antarct. Alp. Res., 36, 156–165, 2004.
Lazzaro, A., Abegg, C., and Zeyer, J.: Bacterial community structure of glacier forefields on siliceous and calcareous bedrock, Eur. J. Soil Sci., 60, 860–870, 2009.
Lazzaro, A., Gauer, A., and Zeyer, J.: A field-scale transplantation experiment to investigate structures of soil bacterial communities at pioneering sites, Appl. Environ. Microb., 77, 8241–8248, 2011.
Le Mer, J. and Roger, P.: Production, oxidation, emission and consumption of methane by soils: A review, Eur. J. Soil Biol., 37, 25–50, 2001.
Liebner, S. and Wagner, D.: Abundance, distribution and potential activity of methane oxidizing bacteria in permafrost soils from the Lena delta, Siberia, Environ. Microbiol., 9, 107–117, 2007.
Ludwig, W., Strunk, O., Westram, R., Richter, L., Meier, H., Yadhukumar, Buchner, A., Lai, T., Steppi, S., Jobb, G., Förster, W., Brettske, I., Gerber, S., Ginhart, A. W., Gross, O., Grumann, G., Hermann, S., Jost, R., König, A., Liss, T., Lüßmann, R., May, M., Nonhoff, B., Reichel, B., Strehlow, R., Stamatakis, A., Stuckmann, N., Vilbig, A., Lenke, M., Ludwig, T., Bode, A., and Schleifer, K.-H.: ARB: A software environment for sequence data, Nucl. Acids Res., 32, 1363–1371, 2004.
Maisch, M., Wipf, A., Denneler, B., Battaglia, J., and Benz, C.: Die Gletscher der Schweizer Alpen: Gletscherhochstand 1850, aktuelle Vergletscherung, Gletscherschwund-Szenarien, vdf Hochschulverlag AG an der ETH Zürich, Zürich, 2000 (in German).
Martineau, C., Whyte, L. G., and Greer, C. W.: Stable isotope probing analysis of the diversity and activity of methanotrophic bacteria in soils from the Canadian High Arctic, Appl. Environ. Microb., 76, 5773–5784, 2010.
Matthews, M. D.: Migration – a view from the top, in: Hydrocarbon migration and its near-surface expression, edited by: Schumacher, D. and Abrams, M. A., Am. Assoc. Petr. Geol., Tulsa, OK, 139–155, 1996.
McDonald, I. R., Bodrossy, L., Chen, Y., and Murrell, J. C.: Molecular ecology techniques for the study of aerobic methanotrophs, Appl. Environ. Microb., 74, 1305–1315, 2008.

Moldrup, P., Olesen, T., Gamst, J., Schjonning, P., Yamaguchi, T., and Rolston, D. E.: Predicting the gas diffusion coefficient in repacked soil: Water-induced linear reduction model, Soil Sci. Soc. Am. J., 64, 1588–1594, 2000.
Moore, T. R. and Knowles, R.: Methane emissions from fen, bog and swamp peatlands in Quebec, Biogeochemistry, 11, 45–61, 1990.
Muller, R. N. and Hamilton, M. E.: A simple, effective method for determining the bulk density of stony soils, Commun. Soil Sci. Plan., 23, 313–319, 1992.
Nauer, P. A. and Schroth, M. H.: In situ quantification of atmospheric methane oxidation in near-surface soils, Vadose Zone J., 9, 1052–1062, 2010.
Nemergut, D., Anderson, S., Cleveland, C., Martin, A., Miller, A., Seimon, A., and Schmidt, S.: Microbial community succession in an unvegetated, recently deglaciated soil, Microb. Ecol., 53, 110–122, 2007.
Sawstrom, C., Mumford, P., Marshall, W., Hodson, A., and Laybourn-Parry, J.: The microbial communities and primary productivity of cryoconite holes in an arctic glacier (Svalbard 79° N), Polar Biol., 25, 591–596, 2002.
Shrestha, P. M., Kammann, C., Lenhart, K., Dam, B., and Liesack, W.: Linking activity, composition, and seasonal dynamics of atmospheric methane oxidizers in a meadow soil, ISME J., online first: doi:10.1038/ismej.2011.179, 2011.
Sigler, W. V. and Zeyer, J.: Microbial diversity and activity along the forefields of two receding glaciers, Microb. Ecol., 43, 397–407, 2002.
Sims, G. K., Ellsworth, T. R., and Mulvaney, R. L.: Microscale determination of inorganic nitrogen in water and soil extracts, Commun. Soil Sci. Plan., 26, 303–316, 1995.
Smith, K. A., Dobbie, K. E., Ball, B. C., Bakken, L. R., Sitaula, B. K., Hansen, S., Brumme, R., Borken, W., Christensen, S., Priemé, A., Fowler, D., Macdonald, J. A., Skiba, U., Klemedtsson, L., Kasimir-Klemedtsson, A., Degórska, A., and Orlanski, P.: Oxidation of atmospheric methane in northern European soils, comparison with other ecosystems, and uncertainties in the global terrestrial sink, Glob. Change Biol., 6, 791–803, 2000.
Soil Survey Staff: Soil survey laboratory information manual. Soil survey investigations report no. 45, Version 2.0, edited by: Burt, R., US Department of Agriculture, Natural Resources Conservation Service, Lincoln, Nebraska, 2011.
Stibal, M., Lawson, E. C., Lis, G. P., Mak, K. M., Wadham, J. L., and Anesio, A. M.: Organic matter content and quality in supraglacial debris across the ablation zone of the greenland ice sheet, Ann. Glaciol., 51, 1–8, 2010.

Tchawa Yimga, M., Dunfield, P. F., Ricke, P., Heyer, J., and Liesack, W.: Wide distribution of a novel *pmoA*-like gene copy among type II methanotrophs, and its expression in *Methylocystis* strain SC2, Appl. Environ. Microb., 69, 5593–5602, 2003.

Urmann, K., Gonzalez-Gil, G., Schroth, M. H., and Zeyer, J.: Quantification of microbial methane oxidation in an alpine peat bog, Vadose Zone J., 6, 705–712, 2007.

Wadham, J. L., Cooper, R. J., Tranter, M., and Bottrell, S.: Evidence for widespread anoxia in the proglacial zone of an arctic glacier, Chem. Geol., 243, 1–15, 2007.

Wang, F. L. and Bettany, J. R.: Methane emission from canadian prairie and forest soils under short term flooding conditions, Nutr. Cycl. Agroecosys., 49, 197–202, 1997.

Whalen, S. C. and Reeburgh, W. S.: Consumption of atmospheric methane by tundra soils, Nature, 346, 160–162, 1990.

Whalen, S. C., Reeburgh, W. S., and Barber, V. A.: Oxidation of methane in boreal forest soils: A comparison of seven measures, Biogeochemistry, 16, 181–211, 1992.

Yavitt, J. B., Downey, D. M., Lang, G. E., and Sexston, A. J.: Methane consumption in two temperate forest soils, Biogeochemistry, 9, 39–52, 1990.

Yergeau, E., Hogues, H., Whyte, L. G., and Greer, C. W.: The functional potential of high arctic permafrost revealed by metagenomic sequencing, qPCR and microarray analyses, ISME J., 4, 1206–1214, 2010.

Zheng, Y., Yang, W., Sun, X., Wang, S.-P., Rui, Y. C., Luo, C. Y., and Guo, L. D.: Methanotrophic community structure and activity under warming and grazing of alpine meadow on the Tibetan Plateau, Appl. Microbiol. Biot., online first: doi:10.1007/s00253-011-3535-5, 2011.

Table 1. Overview of sampled glacier forefields and site characteristics. Soil age is reported in sampling sequence for each location.

Glacier	Site abbrev.	Coordinates WGS84 N	Coordinates WGS84 E	Altitude (terminus) m a.s.l.	Average rainfall[a] mm y^{-1}	Bedrock type	Sampling dates in 2010 (no. of locations)	Maximum soil age[b] (yr)
Unterer Arolla	BAR	45°59′52″	7°29′39″	2150	727	siliceous	30.07. (4)	20,20,20,10
Damma	DAM	46°38′10″	8°27′24″	2100	1559		12.10. (4)	20,20,20,20
Forno	FOR	46°20′20″	9°41′60″	2250	1462		04.07. (5)	5,5,5,20,20
Mont-Miné	MOM	46°02′39″	7°33′12″	2000	727		28.07. (4)	10,10,10,10
Morteratsch	MRT	46°25′45″	9°56′05″	2050	811		03.07. (7)	5,5,5,5,5,20,>50
Stein	STI	46°43′14″	8°26′01″	2000	1661		18.06. (3) 16.07. (1)	10,5,5 10
Steinlimi	STL	46°42′39″	8°24′42″	2200	1661		16.07. (4)	5,5,5,5
Tschierva	TSV	46°24′22″	9°51′48″	2300	811		02.07. (4)	10,10,10,20
Claridenfirn	CLF	46°51′12″	8°55′25″	2600	1802	calcareous	22.09. (3)	5,5,5
Griessfirn	GRF	46°50′37″	8°49′45″	2250	1798		10.08. (4)	20,20,20,20
Griessen	GRI	46°50′52″	8°29′07″	2500	1591		07.07. (4) 04.08. (1)	all >50
Im Griess	KLG	46°51′31″	8°52′23″	2100	1789		09.07. (2) 21.07. (4)	10,10 50,50,>50,>50
Wildstrubel	WIL	46°23′54″	7°33′42″	2600	1099		26.08. (5)	40,40,40,40,10

[a] Data are from the closest precipitation monitoring station of MeteoSwiss (https://gate.meteoswiss.ch/idaweb, last access on 5 December 2011); station overview: http://www.meteoschweiz.admin.ch/web/en/climate/observation_systems/surface.Par.0047.DownloadFile.tmp/listofprecipitationmonitoringnetwork.pdf.

[b] Years since last record of ice coverage, rounded to 5-yr intervals.

Table 2. Overview of physical properties at sampled sites in 0–10 cm soil depth. Soil texture is reported in sequence of sampled locations; for soil temperature, skeleton content, θ_t and S_w, the range of measured values are given.

	Site abbrev.	Soil temperature[a] (°C)	Soil texture[b] (<2 mm)	Skeleton content (>2 mm; wt%)	Porosity θ_t	Water saturation S_w (vol%)
Siliceous sites	BAR	9–13	s, s, ls, s	10–59	0.39–0.52	15–26
	DAM	4–10	s, s, s, s	n.a.	0.38–0.45	7–16
	FOR	8–15	sil, s, s, s, s	2–21	0.46–0.59	2–37[c]
	MOM	15–21	ls, sl, sl, sl	2–36	0.40–0.50	18–34
	MRT	8–22	s, s, s, s, s, s, ls	1–16	0.36–0.57	2–28[c]
	STI	7–17	s, s, s, s	n.a.	0.50[c,d]	20[d]
	STL	20–26	s, s, s, s	6–38	0.40–0.48	7–60
	TSV	15–16	ls, ls, sl, s	14–45	0.41–0.49	4–17[c]
Calcareous sites	CLF	11–14	ls, s, s	17–69	0.46–0.49	1–11[c]
	GRF	14–16	s, s, s, s	18–60	0.36–0.45	9–17
	GRI	8–16	l, sl, l, sl, s	41–95	0.36–0.51	14–35
	KLG	17–20	s, s, s, s, s, ls	2–77	0.42–0.57	5–23
	WIL	12–16	s, ls, ls, s, s	47–62	0.37–0.46	8–23

[a] Range of temperatures measured during sampling.
[b] s = sand; ls = loamy sand; sl = sandy loam; l = loam; sil = silty loam.
[c] Measurements of volumetric water content by TDR.
[d] Data for location 4 only; no data available for location 1–3 n.a. not available.

Table 3. Site mean of measured chemical parameters for each glacier forefield. Values are reported with ±2 sd, which reflects the variance within the site. Organic carbon is not reported, as the difference between TC and IC was below the sd of individual sample replicates. "n.d.": not detected; "n.a.": not available.

	Site		Al	Si	Ca	Fe	P	S	Cu	TC	IC	DOC	NH_4^+	NO_3^-	PO_4^{3-}	SO_4^{2-}
	abbrev.	pH	%				mg (g d.w.)$^{-1}$	µg (g d.w.)$^{-1}$		%	%	µg (g d.w.)$^{-1}$				
Siliceous sites	BAR	6.42 ±0.51	5.31 ±0.85	22.1 ±3.5	1.95 ±0.35	2.56 ±0.57	0.398 ±0.094	<20	6.80 ±3.3	0.035 ±0.016	0.016 ±0.020	30.0 ±6.0	0.313 ±0.55	0.138 ±0.15	0.639 ±0.90	<1.77
	DAM	4.88 ±0.090	4.06 ±1.2	22.6 ±1.5	0.53 ±0.070	0.87 ±0.10	2.15 ±0.079	<20	1.75 ±1.3	0.021 ±0.028	n.d.	70.6 ±24	<0.17	<0.13	n.d.	<1.77
	FOR	7.24 ±0.66	4.52 ±1.2	19.6 ±3.6	2.20 ±1.1	1.71 ±1.0	1.02 ±1.3	<20	5.24 ±4.1	0.083 ±0.075	0.044 ±0.092	33.0 ±34	0.194 ±0.095	0.136 ±0.22	0.537 ±1.5	<1.77
	MOM	7.91 ±1.1	5.01 ±0.14	22.8 ±0.88	1.75 ±0.22	1.90 ±0.31	0.266 ±0.046	34.9 ±41	7.03 ±3.4	0.033 ±0.023	0.018 ±0.032	32.6 ±7.5	<0.17	0.214 ±0.23	2.83 n.a.	4.88 ±4.4
	MRT	6.22 ±1.4	4.36 ±1.1	21.8 ±6.2	1.28 ±1.4	2.06 ±2.0	0.362 ±0.39	<20	5.94 ±3.1	0.026 ±0.022	<0.01	34.6 ±35	<0.17	0.183 ±0.19	1.06 ±2.0	2.20 ±2.2
	STI	7.26 n.a.	5.11 n.a.	22.2 n.a.	1.18 n.a.	2.60 n.a.	0.061 n.a.	<20	21.9 n.a.	0.071 n.a.	0.013	23.8 n.a.	<0.17	0.166 n.a.	n.d.	6.90 n.a.
	STL	6.36 ±0.97	4.38 ±1.0	18.2 ±3.8	0.88 ±0.31	2.29 ±0.19	0.594 ±0.094	<20	11.3 ±4.8	0.020 ±0.011	0.064 ±0.18	44.7 ±42	<0.17	0.154 ±0.31	n.d.	3.99 ±5.5
	TSV	8.33 ±0.22	5.17 ±0.37	22.2 ±1.03	3.18 ±0.83	2.75 ±0.28	0.619 ±0.17	<20	10.5 ±2.4	0.298 ±0.14	0.316 ±0.13	38.4 ±36	<0.17	0.184 ±0.37	n.d.	1.87 ±1.0
Calcareous sites	CLF	8.02 ±0.29	1.66 ±0.21	8.11 ±1.9	24.9 ±3.5	1.90 ±0.32	0.211 ±0.095	51.9 ±34	7.23 ±1.5	7.61 ±1.3	7.43 ±1.1	77.6 ±24	0.717 ±0.51	0.248 ±0.20	n.d.	4.30 ±9.2
	GRF	8.36 ±0.15	3.12 ±1.4	10.4 ±2.6	20.0 ±5.0	2.52 ±0.75	0.161 ±0.063	425 ±410	18.7 ±13	6.67 ±2.1	6.45 ±1.9	70.1 ±5.0	0.551 ±0.29	1.31 ±1.7	n.d.	11.1 ±13
	GRI	8.64 ±0.18	0.410 ±0.13	1.52 ±1.1	36.2 ±2.9	0.430 ±0.32	0.100 ±0.031	117 ±30	4.70 ±1.5	11.4 ±0.66	11.2 ±0.95	32.7 ±34	0.440 ±0.50	0.262 ±0.20	<0.20	3.51 ±5.8
	KLG	8.26 ±0.20	2.11 ±0.67	7.94 ±1.6	25.2 ±3.4	1.90 ±0.38	0.144 ±0.048	136 ±89	10.3 ±2.9	7.84 ±1.2	7.68 ±1.3	22.2 ±1.9	0.690 ±0.45	0.707 ±0.89	2.76 n.a.	13.7 ±18
	WIL	8.55 ±0.36	1.54 ±1.5	9.80 ±1.1	26.5 ±3.4	1.03 ±0.73	0.0917 ±0.085	156 ±88	5.44 ±3.3	8.19 ±0.78	8.17 ±0.81	64.7 ±20	0.272 ±0.20	0.391 ±0.14	n.d.	4.65 ±1.7

Table 4. Number of samples with successful amplification using different primer combinations during normal (first round) and nested (second round) PCR reactions. The second-round PCR was performed with the product of the first-round primer set A189f-A682r. Total number of samples selected for molecular analyses was 27.

PCR reaction	Forward primer	Reverse primer		
		A682r	mb661r	A650r
first round	A189f	17	1	0
second round	A189f		0	0
	pmoA206f		27	0

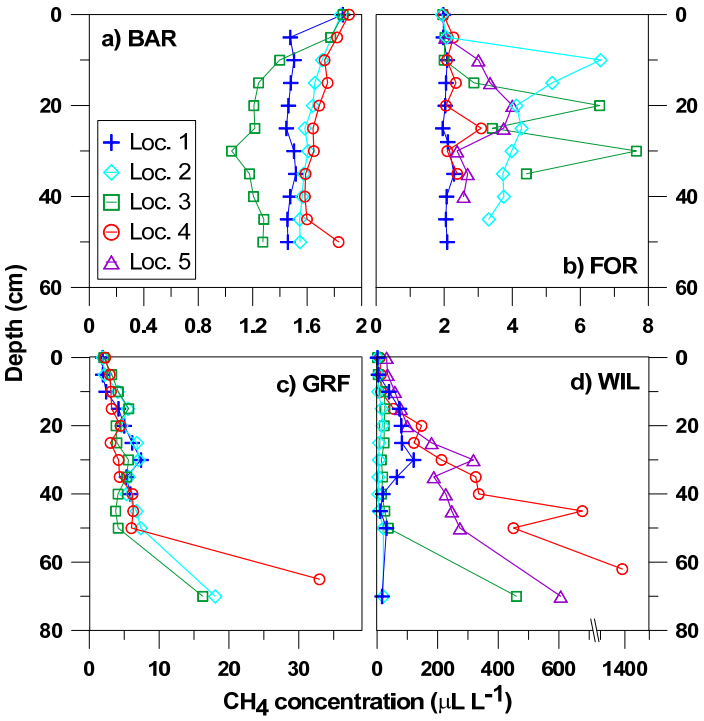

Fig. 1. Selection of measured soil-gas CH_4 concentration profiles representative for the different situations encountered. The legend in plot **(a)** applies to all subplots. Note the different scale in CH_4 concentrations for each site.

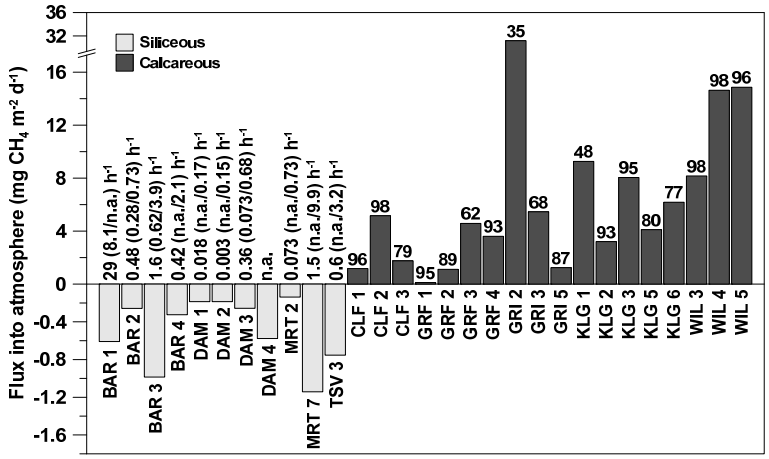

Fig. 2. Fluxes of CH_4 from the soil into the atmosphere (J_{atm}) for locations where the profile shape allowed quantification. Negative J_{atm} indicate that the soil was a sink for atmospheric CH_4. For these locations estimated k of CH_4 oxidation are reported (with low/high 95 % confidence interval). For locations with positive J_{atm}, the number above the bars indicates the percentage of CH_4 oxidized in the soil before reaching the atmosphere. Note that the scale for negative and positive fluxes is different.

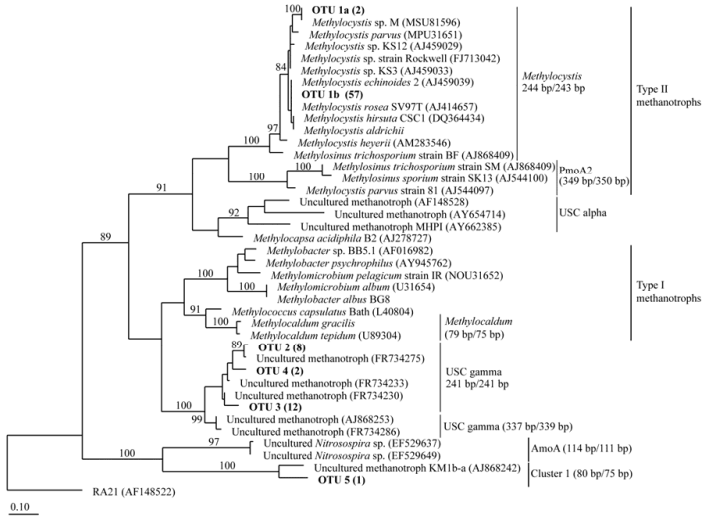

Fig. 3. Maximum-likelihood tree showing the phylogenetic affiliation of *pmoA* sequences obtained from different glacier forefields. The *pmoA* tree was constructed based on 139 derived amino acid sequence positions. Sequences obtained in the course of this study were grouped into 5 species-level units (OTU 1 to 5) based on an amino acid sequence identity threshold of 93 %. The number of clones obtained for each OTU are given in parenthesis. All species-level OTUs also contain published *pmoA* sequences. Predicted T-RF lengths based on MspI are shown on the left side, while the experimental T-RF lengths are indicated on the right side. The in silico predicted T-RF lengths were experimentally confirmed by T-RFLP analysis of individual *pmoA* clone sequences. Bootstrap values greater than 80 are shown (100 replicates). The sequence of RA21 (AF148522) was used as outgroup. The scale bar represents 10 % sequence divergence or 0.1 substitutions per amino acid position.

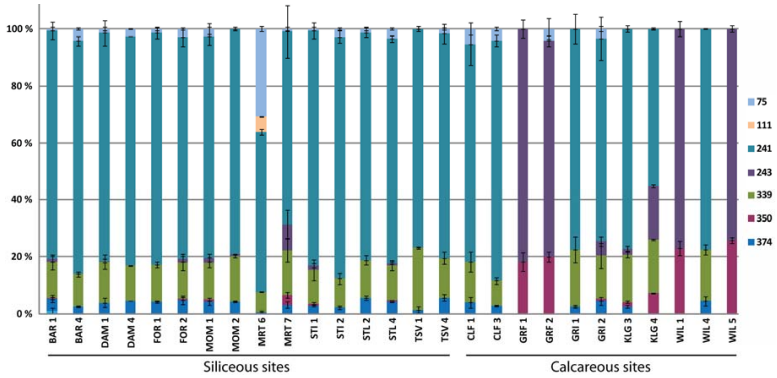

Fig. 4. Bar diagrams of *pmoA*-based T-RFLP fingerprint patterns obtained from all 27 subsamples representing the 13 different glacier forefields. The T-RFLP patterns were generated using the primer set A189f-A682r in first-round PCR and the primer set pmoA206f-mb661 in nested second-round PCR. The percentage abundances (mean ± sd; $n = 3$) of 7 distinguishable T-RFs are indicated by different colors.

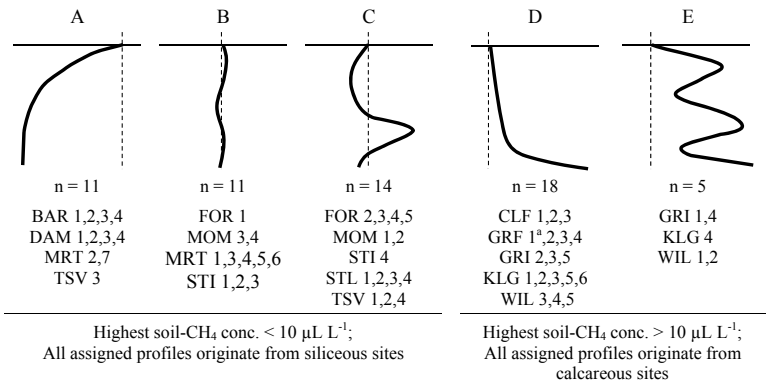

Fig. 5. Qualitative Categories A–E assigned to measured soil-gas CH_4 profiles according to profile appearance. Illustrated profile shapes are typical for each category. The vertical line indicates atmospheric CH_4 concentration. Sampled locations assigned to the respective categories are listed below.